

The peanut pods-associated microbiota and their effects on aflatoxin contamination

Yanpo Yao

Oil Crops Research Institute Chinese Academy of Agricultural Sciences

Qi Zhang

Oil Crops Research Institute Chinese Academy of Agricultural Sciences

Silivano Edson Mwakinyali

Oil Crops Research Institute Chinese Academy of Agricultural Sciences

Suyan Gao

Oil Crops Research Institute Chinese Academy of Agricultural Sciences

Xiaoxia Ding

Oil Crops Research Institute Chinese Academy of Agricultural Sciences

Shuqing Liang

Oil Crops Research Institute Chinese Academy of Agricultural Sciences

Zhongkui Xia

Health Time Institute

Peiwu Li (✉ peiwuli@oilcrops.cn)

<https://orcid.org/0000-0003-1479-2427>

Research

Keywords: Peanut, aflatoxin contamination, microbiota, environmental factors, metagenome, structure, function

Posted Date: January 17th, 2020

DOI: <https://doi.org/10.21203/rs.2.21090/v1>

License:  This work is licensed under a Creative Commons Attribution 4.0 International License. [Read Full License](#)

Abstract

Background: Aflatoxin, which is highly carcinogenic and toxic, can seriously threaten the quality and safety of agricultural products, is mainly produced by *Aspergillus flavus*, which mainly exists in the soil of farmland. However, the correlation between aflatoxin, the microflora and environmental factors that survive in the roots of the plant is currently unknown. In this study, we used peanut-associated microbial populations as a model to address these issues.

Results: We illustrated here that peanut pods significantly enriched with fungi and bacteria phyla. In the aflatoxin low pollution area, fungal and bacterial were more abundant than the high-pollution area, and the proportion of bacterial populations negatively correlated with aflatoxin was higher. However, some functions related to microbial-microbial and plant-microbial interactions were significantly enriched in areas with low levels of aflatoxin. Besides, we found that pH, Fe, Zn, P of the soil and temperature and humidity were the main factors that caused the differential composition and functional characteristics of microorganism. They can significantly affect the relationship between microbial flora and *Aspergillus flavus* and positively regulate aflatoxin production and microbial metabolism pathways, while OM, K, and other elements negatively regulated aflatoxin production and microbial metabolism pathways.

Conclusions: The abundance of *Aspergillus flavus* and aflatoxin are significantly regulated by the population structure and function of microbiota, and this regulation is primarily affected by soil physical and chemical properties. Our results provide novel insights for understanding the contributions of the community enrichment process of the peanut pod-associated microbiome to the peanut hosts.

Background

As an important part of soil, microorganisms inhabiting the rhizosphere, rhizoplane and root endosphere are important symbionts of host plants [1–5]. These symbionts together with the microenvironment around form a unique micro-ecological flora, constituting a comprehensive ecological unit for plants [3]. The effects of these symbiotic microbiota interactions on plants' adapting to environments have been widely noted for more than a century [6]. Many researchers have studied the possibility and molecular mechanisms of utilizing the symbiotic relationships between plants and microbiota for disease control [7–10]. However, technical limitations and insufficient depth of sequencing constrained the analysis of microbiota related to plant growth, disease resistance, and environmental adaptability [8, 9]. Nowadays, the novel high-throughput sequencing technology has facilitated the investigation of plant-associated microbiome and provided a glimpse of microbial diversity [9]. Recent studies of symbiotic microbiota have revealed a profound physiological impact on the host plants, demonstrating a strong relationship between microbiome structure and environmental factors, plant diseases, and even hosts innate systems [10–12].

The effects of symbiotic microbiota on the physiology and fertility of host plants have been fully described [13]. Root-associated microbiome changes due to soil type, geographical location and inhabiting niches, which can significantly affect plant production, health and system-maintenance capabilities [14], such as stress resistance and adaptability, assimilation and absorption, metabolism and carbon fixation, as well as self-repair abilities [15–20]. However, the complexity of taxonomy and genetic diversity of microbial populations hinders the illustration of the functional properties and potential utility of microbiota [21]. But, the previous studies mainly analyzed the influence of plant genetic background and environmental conditions on the plant diseases [6–8], but how environmental conditions affect the production of toxins by some microorganisms (such as *A. flavus* and aflatoxin) and how to adjust the structure and function of microbial population is still very limited, which may significantly affect the control of biotoxin pollution and the quality and safety of agricultural products. Also, research on toxin-producing fungi has mainly focused on above-ground parts of plants such as corn, rice, barley, wheat, soybeans, rape, olives, nuts, and fruits. Compared with the above-ground part of the plant [22, 23], the underground growth part of the plant has a more complex microbiota and ecological environment, and the relationship between the ecological environment, microbial population, and mycotoxins has been rarely studied. Here, we investigated the population structure, diversity, and assembly process of microorganisms associated with peanut pods, soil environmental conditions, and the relationship between the microbiome and *A. flavus* and aflatoxin.

Aflatoxin is a type of secondary metabolite produced by *A. flavus* and *A. parasiticus*. It mainly includes six major classes of aflatoxin B₁, B₂, G₁, G₂, M₁, and M₂. It has acute and chronic toxicity, carcinogenicity, mutagenicity, and teratogenicity, of which aflatoxin B₁ is the most toxic. Its toxicity is 10 times higher than that of potassium cyanide, 68 times than that of arsenic, and 10,000 times than that of hexachlorocyclohexane. It has been identified as a type I carcinogen by the World Health Organization (WHO) [22, 23]. Peanuts are the most susceptible to *A. flavus* and aflatoxin contamination. Every step from planting to consumption may be contaminated by *A. flavus*, causing great harm to human and animal health [22].

The research found that there is a close relationship between *A. flavus* and soil microorganisms, but the research on the correlation between aflatoxin pollution and soil microbial community structure and functional specificity is unknown [24]. Our previous results suggested that the population abundance of *A. flavus* is closely related to the microbial community in peanuts and can significantly change the microbial population structure of fungi associated with the soil. However, the low-throughput-based methods applied in these previous studies have limited our understanding of the structure and diversity of peanut microbial populations. In addition, these studies have mainly focused on fungal populations that colonize the rhizosphere or on the surface of pod shell. How *A. flavus* and aflatoxin affect the population structure, diversity and assembly process of microbiota, and how it affects the function, especially of microbiota that are closely related to the healthy growth of peanuts, is still unclear.

In this study, using 16S, ITS, and metagenomic technologies, we obtained the details of the peanut-pod-associated microbiome, investigated the population structure, diversity, and functions of the microbiota inhabiting on the surface of the shell and in the shell of the peanut, and clarified the relationship between *A. flavus* and microbial population and function of peanut pods. In addition, the results of the study found that soil environment and climatic factors are important driving forces affecting the production of aflatoxins and its relationship with pod-associated microbiota.

Results

The structure and diversity of peanut pods-associated microbiome

We collected samples from 6 major peanut-growing areas in China, including Zhanjiang in Guangdong Province (ZJ for short, 21.1131°N, 110.2259°E), Zhangshu in Jiangxi Province (JZ for short, 27.9346°N, 115.3114°E), Hong'an in Hubei Province (HH for short, 30.9612°N, 114.6454°E), Linyi in Shandong Province (SL for short, 34.9198°N, 118.6507°E), Tangshan in Hebei Province (HT for short, 39.7669°N, 118.6469°E) and Fuxin in Liaoning Province (LF for short, 42.0117°N, 121.4013°E) (Additional file 1: Figure S1A). We collected 215 microbial samples either in the peanut shell or on the surface of peanut shell from the aforementioned areas, of which 143 samples were used for ITS (internal transcribed spacer) analysis specifically for fungi, and 72 on-the-surface-of-peanut-shell samples were used for bacterial 16S rRNA (ribosomal RNA) analysis. The sequencing results contained 5,352,019 fungal ITS tags of high-quality, with an average of 37,426 tags per sample, and a total of 1,884 fungal OTUs (operational taxonomic units) (Additional file 2: Table S1,2). Meanwhile, we obtained 2,716,463 high-quality bacterial 16S tags, with an average of 37,728 tags per sample, from which the clustering annotations totaled 15,648 OTUs (Additional file 2: Table S3,4).

Regardless of sampling sites or inhabiting niches, Ascomycota was the most abundant fungal species associated with peanuts, accounting for more than 80% of the total taxonomic species, followed by Basidiomycota. Other fungal species such as Mucoromycota, Chytridiomycota, Rozellomycota and Glomeromycota occupied a lower abundance in peanut shell-associated niches (Additional file 1: Figure S1B). Different planting regions have significant effects on the relative abundance of fungi on the shell surface or in the shell of peanuts. The relative abundance of the 8 phyla and 159 genera of on-the-shell surface fungi were significantly different between planting regions (Additional file 2: Table S5), while fungi of only 4 phyla and 61 genera in the peanut shell showed significant differences (Additional file 2: Table S6). Ascomycota, Mucoromycota, Chytridiomycota, Rozellomycota, Glomeromycota and Cercozoa were significantly enriched in the peanut shell or on the surface of peanut shell in the southern region, while only Ascomycota and Zygomycota were significantly enriched in the LF and SL of the northern region. Notably, the abundance of Basidiomycota in the shell and on the surface of peanut shell in ZJ and JZ was significantly higher than that in LF, HT and SL, which is consistent with the heavy burden of Basidiomycetes-causing peanut disease in these two areas (Additional file 1: Figure S1B; Additional file 2: Table S5,6; Kruskal-Wallis test, adjusted P-value < 0.05). The reasons for the differences in specific fungi may be due to physical and chemical properties of soils or micro-ecological environments in different regions.

Throughout all sampling areas, bacteria such as Actinobacteria, Proteobacteria, Firmicutes, Chloroflexi, Acidobacteria and Bacteroidetes dominated on the surface of peanut shell (Additional file 1: Figure S1C). Similarly, different planting regions have a significant effect on the relative abundance of bacteria on the shell surface, where 32 phyla and 397 genera of bacteria enriched distinctively in different regions. Acidobacteria, Firmicutes, Chloroflexi, Cyanobacteria and Gemmatimonadetes were significantly enriched in HH, ZJ and JZ of the southern region, while the peanuts in the northern region were mainly enriched in Actinobacteria, Proteobacteria, Bacteroidetes and other bacteria (Additional file 1: Figure S1C; Additional file 2: Table S7; Kruskal-Wallis test; adjusted P-value < 0.05). Most of the fungal and bacterial species were consistent in the 6 peanut-growing areas in China, which may be due to the conserved microbiota associated with peanuts. Interestingly, the results also indicated that the southern peanut-planting areas and the northern planting areas in China represented two distinct microbial communities; besides, in-the-peanut-shell and on-the-surface-of-peanut-shell exhibited two different micro-ecological niches (Additional file 1: Figure S1B,C). We define core species inhabiting in the peanut shell or on the surface of shell as those significantly enriched in different peanut-planting areas with abundance greater than 0 in more than 80% of all the samples. Three core in-the-shell fungi OTUs were *Fusarium oxysporum*, *Talaromyces marneffeii* and *Penicillium levitum*, while three core on-the-shell fungi OTU were *Talaromyces marneffeii*, *Clonostachys rosea* and *Arthrobotrys microscaphoides*. Notably, *Talaromyces marneffeii* was shared by both in-the-shell and on-the-shell samples (Additional file 1: Figure S1B; Additional file 2: Table S8). In total, 87 core bacterial OTUs were found in the on-the-shell soil samples. These core bacteria were mainly concentrated on the bacteria phyla such as Proteobacteria, Bacteroidetes and Actinobacteria (Additional file 1: Figure S1C; Additional file 2: Table S9). From the annotated genera, some core microorganisms may be potential plant-associated probiotics, such as *Bradyrhizobium*, *Novosphingobium*, *Sphingomonas*, *Burkholderia*, *Bdellovibrio* and *Chitinophaga*. These significant differences showed the diversity of the whole microbiome and of core microorganisms, which also contributes to the health, adaptability and stress resistance of peanuts.

The sampling area was the most important factor affecting peanut pods microbial structure and diversity. The box plot of Chao1 index, which depicts alpha diversity, showed the difference in the richness of the species' composition of different sampling regions. Regardless sampling on the shell surface or in the shell, the richness of fungi and bacteria species in different planting regions was significantly different (Fig. 1a-c; Kruskal-Wallis test; P-value < 0.05). Principal Co-ordinates Analysis (PCoA) was performed on the Unweighted Unifrac distance, which is the beta diversity, and showed that clustering either based on fungal or bacterial species, the samples were significantly different due to geographic locations (high aflatoxin contamination areas to low aflatoxin contamination areas), or due to ecological niches (in the shell or on the surface of peanut shell) (Fig. 1c,d). Clearly, both alpha and beta diversity analyses confirmed that the most obvious distinctions of microbiome composition were due to different sampling areas; moreover, on-the-surface-of-peanut-shell and in-the-shell encompass two different ecological niches.

Effects of environmental factors on peanut-associated microbiota

Based on the inter-regional comparison of the microbiome structure and diversity, we found that the differences between different regions were very significant. In order to evaluate the effects of various environmental factors on microbiome structure and diversity, we examined physical and chemical properties of soils in the 6 peanut-planting areas, such as organic matter, nitrogen, phosphorus, potassium, copper, manganese, iron, zinc and pH values, etc., and collected climate data (Additional file 2: Table S10; Additional file 1: Figure S2,3). Next, we performed a permanova analysis to discover a significant correlation between various environmental factors and microbiome structure, and we found that these environmental factors can affect microorganisms such as fungi and bacteria on the shell surface and in the shell of peanuts (Table 1). Average_surface_temperature and Air_temperature can significantly affect the composition of bacteria and fungi on the surface of peanut shell and in the shell (Significance, Average_surface_temperature > Air_temperature), and Aaverage_relative_humidity can only affect the fungal community composition in the peanut shell; and Altitude, Average_rainfall, Average_wind_speed, Sunlight_intensity, Air_pressure had no significant effect on the bacteria and fungi on the shell surface or in the peanut shell. Aflatoxins in the soil

(Significance, Soil_AFB1_total > Soil_AFB1_num > Soil_AFB1_each) and aflatoxins in the peanut shell can both significantly affect the composition of bacteria and fungi on the surface or in the peanut shell. At the same time, the chemical elements (Significance of the ability to affect the composition of bacterial communities: pH > P > Fe > K > Mn > OM > Cu > Zn > N; significance of the ability to affect the composition of fungal communities: OM > pH > P > K > Fe > Mn > Cu > N > Zn) can also significantly affect the bacterial and fungal community composition on the surface and in the peanut shell. In addition, the RDA analysis showed that based on the bacterial or the fungal composition on the surface of peanut shell, Mn, Fe, P, and Zn have a strong positive correlation with the samples with high aflatoxin, and K, PH, Cu, and N have a strong positive correlation with the samples with low aflatoxin; based on the bacterial and fungal community in the peanut shell, the OM (organic matter) and ZJ samples (high aflatoxin) exist a strong negative correlation. Based on the fungal community in the peanut shell, the OM and LF samples (low aflatoxin) had a strong positive correlation (Fig. 2).

Table 1

Permanova test results of various physical and chemical factors on the community composition (OTU levels) of fungi (in the shell and on the surface of the bacteria (on the surface of the shell)).

ID	16S (T)			ITS (T)			ITS (K)				
	F.Model	R2	Pr(>F)	F.Model	R2	Pr(>F)	F.Model	R2	Pr(>F)		
Altitude	0.702	0.149	0.731	1.07	0.211	0.444	1.305	0.246	0.17		
Average_surface_temperature	1.803	0.311	0.025	*	2.139	0.348	0.008	**	1.711	0.3	0.00
Average_rainfall	1.664	0.294	0.065	.	1.745	0.304	0.053	.	1.237	0.236	0.24
Average_wind_speed	0.786	0.164	0.643		0.648	0.139	0.814		1.167	0.226	0.28
Sunlight_intensity	1.043	0.207	0.404		1.085	0.213	0.4		1.03	0.205	0.47
Air_pressure	0.561	0.123	0.874		0.556	0.122	0.911		0.754	0.159	0.78
Air_temperature	1.781	0.308	0.033	*	2.116	0.346	0.008	**	1.643	0.291	0.01
Aaverage_relative_humidity	1.618	0.288	0.101		1.798	0.31	0.04	*	1.47	0.269	0.05
latitude	2.006	0.334	0.013	*	2.292	0.364	0.003	**	1.531	0.277	0.03
group	13.496	0.506	0	***	11.262	0.464	0	***	4.878	0.27	0
Soil_AFB1_num	9.072	0.115	0	***	6.893	0.091	0	***	6.065	0.08	0
Soil_AFB1_total	9.707	0.122	0	***	6.966	0.092	0	***	5.651	0.075	0
Soil_AFB1_each	2.937	0.04	0.002	**	2.761	0.038	0	***	2.194	0.03	0.00
aflatoxin	6.211	0.081	0	***	5.067	0.068	0	***	3.477	0.047	0
OM	8.277	0.107	0	***	6.589	0.088	0	***	6.669	0.088	0
N	3.0499	0.0423	0.0001	***	2.4703	0.0351	0.0002	***	1.8458	0.0261	0.00
P	11.727	0.145	0	***	5.358	0.073	0	***	5.48	0.074	0
K	8.692	0.112	0	***	4.825	0.066	0	***	4.935	0.067	0
PH	12.259	0.151	0	***	5.489	0.075	0	***	5.601	0.075	0
Cu	7.078	0.093	0	***	3.601	0.05	0	***	3.668	0.05	0
Mn	8.434	0.109	0	***	4.144	0.057	0	***	4.258	0.058	0
Fe	10.999	0.137	0	***	4.766	0.066	0	***	4.873	0.066	0
Zn	5.814	0.078	0	***	1.637	0.024	0.037	*	1.666	0.024	0.03

Next we analyzed the correlation between the amount of aflatoxin and the abundance of *A. flavus* (permanova) against the fungi and bacteria species that were significantly different between the aflatoxins high contamination areas and low contamination areas, and the abundance of *A. flavus* in the soil, total and average aflatoxin in the soil, average aflatoxin and abundance of *A. flavus* in the peanut pods (Additional file 1: Figure S4). The results showed that the fungal genus that significantly enriched in the shell and on the surface of the peanut shell in the south has a significant positive correlation with aflatoxin. Besides, the bacteria genus that significantly enriched in the peanut shell in the south also positively correlated with aflatoxin. *A. flavus* highly pollutes the southern region. At the same time, based on the correlation results of significantly different species between aflatoxin-high and low regions, there was a good agreement between the amount of aflatoxin in the pods and the abundance of *A. flavus* in the soil, the total amount of toxin produced, and the *Aspergillus* genus in the soil. *Anaeromyxobacter*, *Bdellovibrio*, *Rhodoplanes*, *Gemmatimonas*, and on-the-surface *Leptospora* are positively correlated with aflatoxin-related indicators (at least with 3 aflatoxin-related indicators with correlation coefficients higher than 0.6). There was a significant negative correlation between *Leifsonia*, *Devosia*, *Exophiala*, on-the-surface *Exophiala* and aflatoxin-related indicators (at least 3 aflatoxin-related indicators with correlation coefficients lower than -0.6).

Then we analyzed the correlation between the amount of aflatoxin and the abundance of *A. flavus* (permanova) against the fungi and bacteria species that were significantly different between the aflatoxin high contamination areas and low contamination areas, and the abundance of *A. flavus* in the soil, total and average aflatoxin in the soil, average aflatoxin and abundance of *A. flavus* in the peanut pods (Supplementary Fig. 4). The results indicated that there was a significant positive correlation between the fungi and bacteria enriched in HH, JZ, and ZJ and *Aspergillus flavus* and aflatoxins. The fungi and bacteria that significantly enriched in HT, SL, and LF negatively correlated with *A. flavus* and aflatoxins. A large number of previous studies have shown that the 3 peanut-planting areas of HH, JZ, and ZJ are areas with high levels of *Aspergillus* infection and aflatoxin contamination [22]. The results of this study can pave the road for the establishment of early warning, prevention, and control measures.

Functional characteristics of peanut pods-associated microbiota

The results above analyzed the population structure and diversity of peanut-associated microbiota in 6 planting areas. To further evaluate the functions of peanut-associated microbiota and the influence of various environmental factors, we collected 22 inter-shell soil samples from the 6 planting areas and conducted metagenome sequencing with an average data volume of 10.7G. After assembling the data with MegaHit, we obtained 30,507,030 contig sequences, and the assembly rate of each sequencing sample reached $15 \pm 7\%$. Through gene prediction and de-redundancy, we finally obtained 41,638,588 UniGenes with an average length of 315 bp (Additional file 2: Table S11). Then, we aligned UniGene sequences to the KEGG gene database using Diamond blastp software, and 21.61% of UniGenes (8,998,131 UniGenes) corresponded to specific KEGG orthology (KO) functions, with 10.98% of UniGenes annotated to metabolism-related pathways. Based on the level2 classification of the KEGG pathway database, we compared the accumulating abundance of genes annotating into each pathway and found that there was no significant difference in gene abundance between the 6 planting regions (Additional file 1: Figure S5A). The top 5 pathways with most genes annotated were metabolism-related pathways, accounting for 50% of the total abundance (Additional file 1: Figure S5A). Furthermore, gene abundance and KO analysis also described the functional differences of microbiomes between the 6 planting regions. We compared the shared and unique KOs in the 6 regions (Additional file 1: Figure S5B) and found that they were very conservative, with a total of 9,064 shared KOs accounting for 92% of total KOs. Among all the 14,937 KOs annotated, 7,335 KOs, almost 50% of the total, were shared by all the samples, thus considered as the core KOs, further illustrating the high conservation of microbial functions in the 6 major regions. Moreover, we performed pathway enrichment and gene abundance analysis of core KOs at the level 2 and level 3 classification of KEGG pathways (Additional file 1: Figure S5C; Additional file 2: Table S12). The results again showed that the most significantly enriched pathways of core KOs were concentrated on the metabolism-related pathways, of which Carbohydrate metabolism, Amino acid metabolism, Energy metabolism, Xenobiotics biodegradation and metabolism were all drastically significant (Fisher's exact test; adjusted P-value < 0.05). Based on the level 3 classification, additional metabolism-related pathways were significantly enriched, such as Microbial metabolism in diverse environments, Biosynthesis of antibiotics, Biosynthesis of secondary metabolites, Butanoate metabolism, Amino sugar and nucleotide sugar metabolism (Additional file 2: Table S12; Fisher's exact test; adjusted P-value < 0.05) and other microbial-microbial interactions and plant-microbial interaction-related metabolism pathways were also significantly enriched, including ABC transporters, Two-component system, Flagellar assembly, Bacterial secretion system, Bacterial chemotaxis, Lipopolysaccharide biosynthesis (Additional file 2: Table S12; Fisher's exact test; adjusted P-value < 0.05).

At the species level, we found that various environmental factors significantly affected the structure and diversity of microbiota inhabiting on the shell surface and in the shell of peanuts. To evaluate the effects of these environmental factors on the functions of these microbial groups, we performed permanova analysis of environmental factors with the overall functions of microbiota. Interestingly, we found that the overall impact of environmental factors on the functions of these microbes was not significant (Additional file 2: Table S13). Therefore, although the structure of peanut shell-associated microbiota in different regions was significantly different due to various environmental factors, their overall functions were highly conserved, to adapt to the similar micro-ecological environments associated with peanuts. While there was no difference in overall functions of microbiota, some special KOs still differed significantly between different regions (Additional file 2: Table S14; Additional file 1: Figure S3). In HH these distinct KOs were significantly enriched in Photosynthesis-antenna proteins and Two-component system (Additional file 2: Table S15; Fisher's exact test; adjusted P-value < 0.05). In JZ the significantly enriched KOs were mainly concentrated on the Lipopolysaccharide biosynthesis pathway (Additional file 2: Table S16; Fisher's exact test; adjusted P-value < 0.05). In ZJ the most abundant KOs were mainly enriched in metabolism-related pathways such as Methane metabolism, Pyruvate metabolism, Carbon fixation pathways in prokaryotes, Glycolysis/Gluconeogenesis, Nitrogen metabolism and Oxidative phosphorylation (Additional file 2: Table S17; Fisher's exact test; adjusted P-value < 0.05). In HT the significantly different KOs were concentrated on Aminoacyl-tRNA biosynthesis, Pentose phosphate pathway, Microbial metabolism in diverse environments, Biosynthesis of amino acids pathway (Additional file 2: Table S18; Fisher's exact test; adjusted P-value < 0.05). In LF the enriched KOs were mainly concentrated on ABC transporters, Flagellar assembly, Phosphotransferase system and Oxidative phosphorylation pathway (Additional file 2: Table S19; Fisher's exact test; adjusted P-value < 0.05). In SL the KOs significantly enriched were mainly Bacterial secretion system (Additional file 2: Table S20; Fisher's exact test; adjusted P-value < 0.05). Our in-depth functional analysis of microbiota and their specifically enriched metabolism-related pathways in different peanut-planting areas revealed that the peanut-associated microbiota in the high-latitude north, especially in LF, were mainly enriched in metabolism pathways closely related to microbial-microbial, microbial-plant interactions. The profound effects of the microbiota on plants in the north were dramatically different from those of the microbiota in the low-latitude south. The structural and functional differences between microbiota may be related to the occurrence of peanut diseases and some mycotoxin contamination.

PCoA analysis based on the bray distance at the gene and KO levels (Additional file 1: Figure S6A, B), we found that there were significant differences between the southern and northern samples (ie, the level of aflatoxin) (permanova test, gene level: pvalue = 0.0001; KO level: pavlue = 0.0001). This was consistent with the amplicon results in the previous section (Fig. 1c,d), indicating that the level of aflatoxin might affect the functional metabolism of the microbial community. RDA analysis based on the physical and chemical indicators (OM, Fe, P, Zn, Mn, K, pH, N) at the KEGG level3 and KO levels (Additional file 1: Figure S6C,D) showed that Fe, P, Zn, and Mn indicators were significantly enriched in the southern samples (HH, JZ, and ZJ), suggesting a positive regulatory effect on aflatoxin production. The K, OM, PH, N indicators were significantly enriched in northern samples (LF, HT, and SL), indicating that these indicators may have a negative regulatory effect on aflatoxin production. This was also consistent with the results of amplicon sequencing samples (Fig. 2).

The relationship between *Aspergillus flavus* and peanut pods-associated microbiota

Whether through the relative abundance analysis of aflatoxin in peanuts from different planting areas or the determination of aflatoxin associated with peanuts and soil, we found that the abundance of *A. flavus* and aflatoxin showed a trend of high in the south and low in the north (Additional file 1: Figure S3). To find the microbial species associated with *A. flavus* and aflatoxin, we used the R language *corrplot* package and the Spearman correlation analysis for *Aspergillus* with other fungal and bacterial genera. Remarkably, as many as 60% of on-the-shell-surface bacteria were significantly negatively correlated with *A. flavus* and aflatoxin, which may be potential *A. flavus* antagonists. Further selection of negatively correlated fungal and bacterial species with higher correlation coefficients, we found that the fungi *Exophiala* and *Guehomyces* inhabiting either on the surface of peanut shell or in the shell were significantly negatively correlated with both *A. flavus* and aflatoxin. Other fungal species, such as *Cladophialophora*, *Trechispora*, *Fusarium*, *Lectera*, etc., were also significantly negatively correlated with *A. flavus* and aflatoxin. Meanwhile, we found that *Brevundimonas*, *Defluviicoccus*, *Devosia*, *Dyadobacter*, *Flavobacterium*, *Methylobacterium*, *Methylotenera*, *Pseudomonas*, *Rhizobium* and other bacteria were negatively correlated with *A. flavus* and aflatoxin (Additional file 2: Table S21,22). These species, especially *Pseudomonas*, *Rhizobium*, *Exophiala*, *Guehomyces* and *Devosia*, may be potential *A. flavus* antagonists. Except for the potential antagonists, we found that more in-the-shell fungi (more than 86% of 45) were significantly positively correlated with *A. flavus*, which may play a beneficial role in the growth of *A. flavus*. Our previous experiments demonstrated the antagonism of *Trichoderma* and *Bacillus* with *A. flavus* [25–27], consistent with our correlation analysis. To further search for fungi and bacteria associated with these known antagonists, we also performed a correlation analysis between antagonists and other microorganisms associated with peanuts. We found that 53 genera of in-the-shell and 101 genera of on-the-shell-surface fungi were significantly correlated with *Exophiala*, most of which were positively correlated (Additional file 2:Table S23). *Trichoderma* was correlated with 23 genera of in-the-shell and 88 genera of on-the-shell-surface fungi, most of which were positively correlated (Additional file 2:Table S24). *Bacillus* was significantly associated with 109 genera of on-the-shell-surface bacteria, most of which were positively correlated, such as *Streptococcus*, *Carnobacterium*, *Lactococcus* and others (Additional file 2:Table S25). These fungi or bacteria that were positively associated with known antagonists may be potential novel *A. flavus* antagonists. More excitingly, we found that on-the-shell-surface *Exophiala* and *Trichoderma* were positively correlated, and both on-the-shell-surface and in-the-shell *Exophiala* was also positively correlated with *Guehomyces*, further consolidating the potential antagonism against *A. flavus* of these fungi. Clearly, in different peanut-planting areas, there were specific or core species of microorganisms closely related to *A. flavus* and aflatoxin. Based on the abundance of the above-mentioned microorganisms, we can infer the abundance of *A. flavus*, which may facilitate predicting aflatoxin contamination on peanuts and provide scientific and effective prevention and control measures.

The DESeq2 hypothesis test was performed at the levels of bacteria, in-the-shell fungi, and on-the-surface-of-the-shell fungi, and the genera that significantly enriched in different habitats were counted. Then, a spearman correlation analysis was performed between these genera (average species abundance higher than 0.1%, significant correlation between species higher than 0.35 or lower than -0.35.) and a network diagram was drawn (Fig. 4). The number of bacterial species level was significantly higher than that of fungal species. At the bacterial level, the low aflatoxin contamination areas had more abundant species than high areas, and the species were more closely related to each other. At the fungal level, there were more species inhabiting on the surface of peanut shell than those in the shell, but there were no species that are significantly related to *Aspergillus* on the surface of peanut shell, while *Aspergillus* was positively correlated with *Clonostachys*, *Penicillium*, *Nigrospora*, and *Conocybe* in the shell, suggesting a potential mutual benefit between them.

The relationship between *Aspergillus flavus* and function of peanut pods-associated microbiota

In addition to identifying on-the-shell-surface and in-the-shell microbes associated with *A. flavus*, we also performed a correlation analysis between peanut-associated microbial functions and *A. flavus*. We found that 1,417 KOs were significantly associated with *A. flavus*, of which 325 KOs showed negative correlations, and most of the other KOs were positively correlated with *A. flavus* (Additional file 2:Table S26; Fig. 3). These positively correlated KOs were mainly concentrated on the KEGG level2 functional pathways such as Carbohydrate metabolism, Signal transduction, Energy metabolism and Xenobiotics biodegradation and metabolism, while negatively correlated KOs were mainly enriched in Signal transduction, Lipid metabolism, Amino acid metabolism and Membrane transport function (Additional file 2:Table S27). Further on the KEGG level 3 metabolism-related pathways, we found significant correlations between KOs in Carbon fixation pathways in prokaryotes, Microbial metabolism in diverse environments, Pyruvate metabolism, Two-component system, Nitrogen metabolism, Methane metabolism, Glycolysis/Gluconeogenesis, Propanoate metabolism, Citrate Significant enrichment on the cycle and Benzoate degradation (Additional file 2:Table S28; Fisher's exact test; adjusted P-value < 0.05). Negatively correlated KOs were mainly concentrated on metabolism-related pathways such as Biosynthesis of antibiotics, ABC transporters, Biosynthesis of secondary metabolites, Flagellar assemblies (Additional file 2:Table S29).

Different ecological environments promote the corresponding microbiome structure and diversity. The crosstalks between microbial-microbial, microbial-plants and microbial-environment profoundly affect the dynamic balance of microorganisms and the health of plants. The previous analysis showed the structure and diversity of peanut-associated fungi and bacteria in different planting areas were significantly different. We hypothesized that this is a micro-ecological cause of different aflatoxin contamination in the 6 peanut-planting areas. We analyzed the function of microbiota inhabiting on the shell surface or in the shell of peanuts from different planting areas. Although the microbial population and function in different regions were highly conserved, there was still some special functional enrichment in each planting area. The high-latitude northern planting area, especially in LF where aflatoxin pollution was less severe, showed concentration of functional KOs mainly on ABC transporters, Flagellar assembly, Phosphotransferase system (PTS) and Oxidative phosphorylation pathway (Additional file 2:Table S15-20). Further correlation analysis of microbial function and *A. flavus* abundance found that KOs, which were negatively correlated with *A. flavus* and aflatoxin, were also concentrated on these metabolism-related pathways (Additional file 2:Table S29). These observations validated our previous hypothesis, that is, the low abundance of *A. flavus* and aflatoxin contamination in the northern peanut-planting region, such as LF, is associated with these negatively correlated pathways and microbial populations. These findings will have a positive impact on the development of aflatoxin-control technology for peanuts, and will also provide a reference for the cause and control of aflatoxin contamination in other crops.

At the KEGG level 3, we first selected 86 pathways that were significantly related to aflatoxin (correlation coefficient > 0.4 or < -0.4, pvalue < 0.05). Then we performed correlation analysis (permanova) of these significant pathways in the 22 samples with corresponding soil physical and chemical indicators (Fig. 5). The results showed that there was a significant positive correlation between P, Fe, Mn, Zn, and aflatoxin-positive-correlated pathways, and a significant

positive correlation between OM, K, pH and aflatoxin-negative-correlated pathways, consistent with the previous results (Fig. 2; Table 1; Additional file 1: Figure S6) that P, Fe, Mn, and Zn had a positive regulating effect on aflatoxin-high region, while OM, K, and pH have a negative regulatory effect on aflatoxin-low region.

Discussion

In this paper, we used bacterial 16S and fungal ITS high-throughput sequencing technology to describe the structure and diversity of microbiome inhabiting in the peanut shell or on the surface of peanut shell from 6 major planting areas in China. The results indicate that in-the-shell and on-the-shell-surface are two distinct micro-ecological niches, which are independent yet closely related. The microbiota inhabiting in the two niches have significant differences. Ascomycota, Basidiomycota and Actinobacteria are the most abundant fungi and bacteria in the peanut shell from both the high-latitude northern peanut-growing region and the low-latitude southern region. Expectedly, as the latitude of the planting area changes, the enriched fungi and bacteria were significantly different. Fungi including Ascomycota, Mucoromycota, Chytridiomycota, Rozellomycota, as well as bacteria including Acidobacteria, Firmicutes, Chloroflexi, Cyanobacteria were dominant in the peanut shell in aflatoxin high contamination area. On the contrary, the fungi Ascomycota and Zygomycota and bacteria Proteobacteria, Actinobacteria and Bacteroidetes dominate in aflatoxin low contamination area. In addition, previous studies found that the newly harvested peanuts and the long-term stored peanuts have significant distinct microbiota, and the newly harvested ones share similar microbiota to the ones growing in the land, indicating that the microbiota associated with peanuts change corresponding to different growth/harvest stages [28, 29], which is critical for maintaining microbiota adaptation, crop growth and quality of agricultural products (Additional file 1: Figure S1; Additional file 2: Table S5-7). Notably, most of the fungi and bacteria associated with peanuts maintain a high degree of consistency even at different latitudes, which may contribute to the stability of microbiota in different environments and ecological niches. Changes in the ecological environment can profoundly affect the species of microorganisms such as fungi and bacteria, and inevitably drive changes in the structure and diversity of microbiome [30–34]. The population structure and diversity of microorganisms such as fungi and bacteria in different regions vary greatly due to different micro-ecological factors, which is manifested by the alpha and beta diversity analyses (Fig. 1).

Based on the effects of regional differences on peanut-associated microbiota, we evaluated these environmental factors that can change microbiome structure and diversity. The results showed that various physical and chemical factors of soil and climatic factors can significantly impact the microbiota of peanuts such as fungi and bacteria (Table 1). The one-way ANOVA analysis showed that these environmental factors can affect the contamination of *A. flavus* and aflatoxin by affecting the microbiome structure and diversity. This opens up new possibilities for developing new methods to control the contamination of *A. flavus* and aflatoxin in peanuts. By optimizing environmental factors and regulating the structure of peanut-associated microbiota, we can change the abundance of *A. flavus* and aflatoxin to improve crop yield and quality. Several groups have influenced the rhizosphere micro-ecology to change the structure and diversity of rhizosphere microbiome of certain crops to control diseases, and have achieved relatively promising results [35, 36]. However, there are no reports on the regulation of plant microbiota to achieve controlling the contamination of *A. flavus* and aflatoxin. Our next future is to carry out research to control aflatoxin in peanuts through micro-ecological and microbial regulation.

Environmental factors can significantly affect the structure and diversity of microbiome associated with peanuts. To further elucidate their relationships, we used metagenome techniques to assess the effects of these factors on the function of microbiota. Surprisingly, although the 6 major planting areas are geologically diverse, that is across three latitudes with distinct ecological environments and climatic factors, we found that there is no significant difference in the population structure, metabolism-related pathways, and KOs of the peanut-associated microbiota in the 6 main producing areas. The high conservation of the populations and functions of microbiota confirms the stability of peanut-associated microorganisms. Although the microbial population associated with peanuts varies in the planting areas due to different ecological environments, the overall functions of the microorganisms remain highly conserved, which is very important for the stability of microorganisms and the adaptability of plants to the environments. Changes in soil microbial populations and diversity have been found to affect the adaptability of plant and promote their evolution [37]. Such studies have shown that changes in the structure and diversity of microbiome can affect the growth and development of plants, as well as the stability of the microbiota themselves. From our results, although the function, structure, and diversity of peanut-associated microbiota in different planting areas remain highly conserved, some microbial functions are still very different between the 6 regions (Additional file 2: Table S14). By comparing the population structure and KOs of microbiota from different peanut-planting areas, we were surprised to find that in the high-latitude northern region, especially in LF, the microbial KOs concentrate mainly on ABC transporters, Flagellar assembly, Phosphotransferase system (PTS) (Additional file 2: Table S19). These pathways are significantly enriched in microbial-microbial interactions and plant-microbial interaction-related metabolisms, which are associated with plant root colonization, stress tolerance, fitness and microbial stability [38]. LF is the main peanut-producing area in China, and it is also a region with a low abundance of *A. flavus* and less aflatoxin pollution. We speculate that there is a certain correlation between the two, and we have carried out further research. The KOs from the low-latitude southern regions are mainly enriched in energy metabolism-related pathways such as Photosynthesis-antenna proteins, Methane metabolism, Carbon fixation pathways in prokaryotes and Nitrogen metabolism (Additional file 2: Table S15-S17).

The rhizosphere micro-ecology of healthy plants is in a state of mutual restraint and mutual checks and balances. When this equilibrium is in danger, the plants will be in sub-health and even disease [39, 40], manifested by aflatoxin contamination of peanuts in different planting areas. Therefore, we analyzed the relative abundance of *A. flavus* in peanuts and soil from different planting areas in China and evaluated the amount and relative level of aflatoxin production. The results showed that the abundance of *A. flavus* and aflatoxin in peanuts and soil exhibited a trend of increasing from high latitude to low latitude, and JZ in Jiangxi province reached highest (Additional file 1: Figure S3). We carried out an analysis of the correlation between the dynamic changes of *A. flavus* and aflatoxin and the fungi and bacteria genera associated with peanuts. We found that 109 genera of fungi and 171 genera of bacteria in the peanut shell are significantly associated with *A. flavus* (Additional file 2: Table S21), 72 genera of fungi and 134 genera of bacteria are significantly associated with aflatoxin (Additional file 2: Table S22). Surprisingly, more than 60% of the genera closely related to *A. flavus* and aflatoxin are negatively correlated, especially the bacterial genera *Pseudomonas*, *Rhizobium*, *Exophiala*, *Guehomyces*, *Devosia*, etc. and fungi genera *Exophiala*, *Guehomyces*, *Cladophialophora*, *Trechispora*,

Fusarium, Lactaria, etc. We have analyzed the fungal and bacterial genera that are significantly negatively correlated with *A. flavus* and aflatoxin as a model for screening for antagonists. The results are very promising. *Trichoderma koningii*, *Trichoderma harzianum* and *Enterobacter ludwigii*, *Burkholderia cepacia* and *Bacillus subtilis* in *Bacillus* can significantly antagonize against *A. flavus*, especially *Enterobacter ludwigii*, can degrade aflatoxin [25–27]. These findings have opened up new perspectives and provided new ideas for us to discover beneficial microorganisms that can effectively prevent and control *A. flavus* and aflatoxin. To further analyze this relationship between microbial populations, we conducted correlation analysis between these microbes and other microbial species associated with peanuts. We found that most of the fungi in the peanut shell were positively correlated with *Exophiala* and *Trichoderma* (Additional file 2:Table S23). Most of the bacteria in the peanut shell were also positively correlated with *Bacillus* (Additional file 2:Table S25). More interestingly, we found that *Exophiala* is positively correlated with *Trichoderma* and *Guehomyces* both in the peanut shell and on the shell surface. This correlation proves the feasibility of the above-mentioned screening strategy for obtaining antagonists. We further carried out the correlation analysis between *A. flavus* and the functions of microbiota inhabiting either in the peanut shell or on the surface of peanut shell. We found that 325 of the 1417 KOs are significantly negatively correlated with *A. flavus* (Additional file 2:Table S26). These negatively correlated KOs are mainly concentrated on pathways such as the Biosynthesis of antibiotics, ABC transporters, Biosynthesis of secondary metabolites, Flagellar assembly (Additional file 2:Table S29). These findings further validate the above-mentioned hypothesis that the microbial populations and their functions are important reasons for containing the low contamination of *A. flavus* and aflatoxin in the northern LF region. These results are instructive for developing novel aflatoxin-control technology, selecting for better peanut species, and predicting aflatoxin contamination, therefore are of great interest for improving peanut quality and safety.

Conclusions

Peanut production and quality are influenced by symbiotic microbes, which change significantly corresponding to different environmental factors. Here we analyzed the microbiota and their corresponding functions from 6 major peanut-planting areas across three latitudes in China, and illustrated structural characteristics of microbiota associated with different niches of peanut shells under different environmental conditions. Moreover, our work is the first to show that the structure, diversity and function of microbiomes inhabiting on and in the peanut shells are distinctive. We also found that core functional genes and pathways enriched by specific microbiota occupying different niches of peanut shells are closely related to *A. flavus* abundance and aflatoxin production. Therefore, our research indicates that microbial-microbial and environment-microbial interactions contribute to the microbiota structure and function in different niches of peanut shells, which have significant effects on aflatoxin contamination. This knowledge can be translated into a better understanding of disease control and could be used for the production of resilient, healthy peanuts.

Methods

Samples of soil associated with peanut shells collection

We have collected a total of 215 samples in 2016 from 6 major peanut-planting areas in China. The whole root system of peanut plants was harvested at the mature period. The soil samples of in-the-shell and on-the-shell-surface and bulk soil samples, which were more than 10 centimeters away from the plants in each sampled fields, were collected. We excavated the peanut plants from the soil and detached the root systems from the stems. We employed a combination of washing and ultrasound treatments to simultaneously separate the on-the-shell-surface fraction or in-the-shell fraction of soil samples. In parallel, bulk soil controls, exposed to the same environmental conditions, were processed. Then the soil samples were blotted on sterile filter paper, quick-frozen in liquid nitrogen, of which 20 g were stored at -80°C until further use, and 80 g were used for analysis of physical and chemical properties of soil.

DNA sequencing and data analysis

Total DNA from fungi and bacteria was extracted using the E.Z.N.A. Soil DNA Kit (Omega Bio-tek, Norcross, GA, U.S.) kit. The PCR was carried out by using the total DNA as templates, and the PCR product was detected by 2% agarose gel electrophoresis. The cut-out target bands were recovered by AxyPrep DNA Gel Extraction Kit (Axygen Biosciences, Union City, CA, US) and were quantified using QuantiFluor: trademark: ST (Promega, US). The recovered DNA was quantitatively mixed with reagents and subjected to high-throughput sequencing using the Illumina HiSeq 2500 sequencing platform with the PE 250 sequencing strategy. The filtered tags were combined using FLASH [41, 42] software (V1.2.7, <http://ccb.jhu.edu/software/FLASH/>), and the quality control was performed by the Qiime [43] software (V1.9.0, <http://qiime.org/index.html>). The effective tags of all the samples were clustered on the 97% level using the Uparse [43] software (Uparse v7.0.1001, (<http://drive5.com/uparse/>)) to form OTUs. Using the Usearch software [44] to compare the 16S and ITS OTUs against the databases Silva (v128, <http://www.arb-silva.de>) and Unite (<http://unite.ut.ee/index.php>) [45, 46] respectively to obtain annotation information for species (confidence threshold of 0.8). Microbiota diversity was illustrated by the Shannon index value. The Beta diversity of the samples was calculated using the Unweighted UniFrac [47, 48] algorithm based on the UPGMA [49, 50] phylogenetic tree. This method considers the existence of species regardless of their abundance. Based on the unweighted unifracs distance matrix of multiple communities, PCoA analysis can be further performed. RDA [51] analysis is a sorting method, combining the corresponding analysis and multiple regression analysis, based on the single-peak model. It is also called multivariate direct gradient analysis, which is mainly used to reflect the relationship between microbiota and environmental factors.

Metagenomics sequencing and data analysis

All samples were sequenced on the Illumina HiSeq 2500 platform. The raw data of each sample was subjected to the removal of reads with N-containing bases more than 10% of the total, or the reads containing the 15 bp adapter sequences, or reads with a continuum of 30 bp with quantity lower than Q20 (about 20% of total reads) to obtain high quality data (Clean data). The MEGAHIT assembly software [52, 53] was used to iteratively assemble the Clean data to obtain the sequences of the metagenomic scaffold for each sample. Then the Clean data was compared back to the assembled scaffold, and the misaligned reads were mixed according to the geological regions. MEGAHIT performed hybrid assembly and then combined the results of the individual sample assembly with the results of the geological regional hybrid assembly as a final assembly sequence set. Metagenomic gene prediction was performed using

MetaGeneMark software [54, 55], and then de-redundancy using CD-HIT-est software [56, 57] to obtain a non-redundant gene set with a threshold set to 95% similarity. Then, the high-quality data obtained by sequencing each sample is compared with the gene sets after de-redundancy. Next, the relative number of reads corresponding to the gene, the length of the gene, and the number of reads on the total alignment of the sample were compared, and the relative abundance of genes were calculated [58]. Gene functional annotation was performed using the DIAMOND software [59] and we compared gene sets against NCBI's NR database and the KEGG database [60, 61] with the alignment threshold set to $1e-5$ to identify the functions of the genes.

Physical and chemical properties of soil

The content of nutrient elements (effective K, Mg, Cu, Zn, Fe, Mn) in the soil was analyzed by a plasma emission spectrometer (PE company, Optima 7300V). The ICP multi-element standard solution 2 (element content 10 mg/L) was diluted to 10 ppb, 40 ppb, 80 ppb, 120 ppb, 160 ppb, 200 ppb, 240 ppb, 280 ppb, 320 ppb, 360 ppb, 400 ppb. The standard solution was then mixed with 5% HNO₃ in a 25 mL volumetric flask. 2 g of air-dried soil samples was added into a 100 mL digestion tube, 15 mL of HCl (1 + 1) and 5 mL of HNO₃ ($\rho = 1.42 \text{ g / mL}$) were added to solve the soil, and shaken for 30 min. The solution was filtrated, and made up to 100 mL. Under the working conditions of the ICP spectrometer, we first measured the blank solution (5% HNO₃), then separately measured the mixed standard solution of different concentrations to obtain the standard curve, and finally measured the soil filtration solution to obtain the nutrient element content in the soil [62].

Soil organic matter was measured by potassium dichromate method. Weigh 0.05 to 0.5 g of sieved air-dried soil (100 mesh) in a 150 mL triangle flask, add a little solid silver sulfate, and add 5.0 mL 0.8 mol / L heavy chromium Potassium acid solution, add 5 mL of concentrated sulfuric acid, shake well, insert air-cooled tube into the mouth of the flask. Place it on a 220 °C constant temperature electric hot plate. When the liquid in the air-cooled tube rises and begins to return, remove it after holding for 8 minutes. Wash the air-cooled tube with distilled water for multiple times to make the total volume of the solution in the flask reach 60 to 70 mL. Titrate with a standard solution of ferrous sulfate, the color of the solution from orange yellow to blue green to brown red is the end point. At the same time, one or two blank tests are performed, that is, the silica powder with the same quality as the sample is used instead of the soil sample for the test [63].

The total nitrogen in soil was measured with a concentrated sulfuric acid on a 300W electric stove, and the total phosphorus in soil was measured with sodium hydroxide alkali melting method at 720 °C. After obtaining the test solution, Kjeldahl nitrogen, molybdenum blue colorimetry, and flame photometry were used for measurement. The specific method is to weigh (0.3 ± 0.01) g of air-dried soil sample passed through a 100-mesh sieve, put it in the bottom of the polytetrafluoroethylene digestion tube without sticking to the wall. Add 4 mL of concentrated sulfuric acid and shake the mixture. Using a plastic dropper, add 1.2 mL of hydrofluoric acid in three times and shake well. Add 0.3 mL of perchloric acid, plug the digestion tube and screw the cap tightly. Place in an automatic digestion apparatus and digest for 4 hours at 195 °C. Open the digestion instrument and wait for the digestion tube and the test solution in the tube to completely cool down. Then open the lid of the digestion tube, and heat it at 120 °C for 30 minutes on the hot plate to remove hydrofluoric acid. Cool down to a 100 mL volumetric flask and wait for testing.

Examination of aflatoxin in peanut pods

Aflatoxin content was determined by high performance liquid chromatography (HPLC, Agilent 1260 Infinity, USA). Aflatoxin B1 standard, purity 98%, 3 mg/L; aflatoxin B1 standard stock solution: take 1 ml of a concentration of 3 mg/L to a 25 ml volumetric flask, make up to volume with acetonitrile, and mix to obtain the standard solution of 120 µg/L. HPLC conditions: chromatographic column: Waters Symmetry C18 5 µm, 4.6 mm × 250 mm, injection volume: 20 µl, column temperature: 30 °C, flow rate: 1.0 ml/min; mobile phase: acetonitrile: water = 18:82 (volume ratio), fluorescence detection wavelength: excitation wavelength 365 nm, emission wavelength 440 nm. Weigh 5.0 g of sample into a 50 ml centrifuge tube with a lid, add 25.0 ml aflatoxin B1 extract, shake at room temperature for 15 min, centrifuge at 3000 r/min for 5 min, take 1 ml of supernatant in a 10 ml glass test tube, 50 °C water bath, blow dry with nitrogen. For the preparation of standard solutions, accurately transfer 50, 100, 250, 500, 750, and 1000 µl aflatoxin B1 standard stock solutions into 10 ml glass test tubes, and blow dry at 50 °C with a nitrogen blower. Add 350 µl of trifluoroacetic acid, 350 µl of n-hexane to the sample and the standard working solutions, shake for 30 s, and derivatize at room temperature for 15 min in the dark, and finally add 650 µl of acetonitrile-water solution (1: 9), shake for 30 s, and centrifuge at 3000 r/min for 10 min The bottom liquid was filtered and tested on the machine (HPLC).

Statistical analysis

Analysis of the microbiome differences between either geological regions or micro-ecological niches were performed using the Kruskal-Wallis one-way analysis of variance [64], which is also called the Kruska-Wallis test, uses the rank sum of multiple samples to infer whether each sample represents the whole population. We used the `kruskal.test` package in the R language to compare the relative abundance between different groups and also to correct the test hypothesis [65]. When the difference was significant, the group with the largest relative abundance was considered the most significantly enriched. Relative to the blank soil samples, the significantly enriched microorganisms inhabiting in the peanut shell or on the surface of peanut shell were identified using the DESeq2 package for differential analysis of the two data sets [66]. First, the TMM method was used to standardize the samples on the basis of absolute abundance, and then the differential analysis was performed based on the negative binomial distribution model. The microbial species in the peanut shell or on the surface of peanut shell were considered as significantly enriched species if their abundance was greater than those in the blank soil and they showed significant differences between the two micro-ecological niches. The functional enrichment analysis of the species between the 6 geological regions were carried out using the Kruskal-Wallis one-way ANOVA [64] to obtain the enriched KOs. The KEGG enrichment utilized a hypergeometric test to perform pathway enrichments for the differential KOs ($p < 0.05$).

Declarations

Acknowledgements

We thank Ben Niu (Northeast Forestry University) for the comments on this manuscript.

Funding

This work was supported by the national key research and development program of china (2018YFC1602505), National Natural Science Foundation of China (31801665), and The Major Project of Hubei Provincial Technical Innovation (2018ABA081).

Availability of data and materials

Raw sequences can be accessed in the Short Read Archive of NCBI under project no. PRJNA594760. All processed datasets have been deposited in a Zenodo repository <https://zenodo.org/record/3571485>.

Authors contributions

YPY, QZ and PWL designed the experiments, SYG prepared the samples, SQL, ZKX generated the data, YPY, QZ and XXD analysed the results, YPY, SQL and SM wrote the paper. All authors read and approved the final manuscript.

Ethics approval and consent to participate

Not applicable.

Consent for publication

Not applicable.

Competing interests

The authors declare that they have no competing interests.

Publisher's Note

Springer Nature remains neutral with regard to jurisdictional claims in published maps and institutional affiliations.

Authors details

¹Oil Crops Research Institute, Chinese Academy of Agricultural Sciences, Wuhan 430062, China. ²Key Laboratory of Biology and Genetic Improvement of Oil Crops, Ministry of Agriculture, Wuhan 430062, China. ³Key Laboratory of Detection for Mycotoxins, Ministry of Agriculture, Wuhan 430062, China. ⁴Laboratory of Risk Assessment for Oilseeds Products, Wuhan, Ministry of Agriculture, Wuhan 430062, China. ⁵Quality Inspection and Test Center for Oilseeds Products, Ministry of Agriculture, Wuhan 430062, China. ⁶Health Time Gene Institute, Shenzhen, 518000, China.

Additional Files

Additional file 1: **Figure S1.** Microbiota structure associated with peanuts in the 6 major peanut-planting areas. **Figure S2.** Chemical characteristics of the soil from 6 peanut-growing areas in China. **Figure S3.** Abundance and aflatoxin content of *Aspergillus flavus* in the shell and on the surface of shell from 6 peanut-growing areas in China. **Figure S4.** Correlation analysis heat map (permanova) of significantly different species (genus) in the shell and on the surface of peanut shell with *Aspergillus flavus* and its aflatoxins. **Figure S5.** Functional characteristics of on-the-shell-surface microbiota associated with peanuts. **Figure S5.** PCoA & RDA analysis of functional genes and metabolic pathways of peanut-pod-associated microbiota.

Additional file 2: **Table S1.** Fungal tags and OTU number of each sample. **Table S2.** Fungal OTU abundance table and annotation in the last column. **Table S3.** Bacteria tags and OTU number of each sample. **Table S4.** Bacteria OTU abundance table and annotation in the last column. **Table S5.** Statistics of fungi phyla and genera on the surface of peanut shell. **Table S6.** Statistics of fungi phyla and genera in the peanut shell. **Table S7.** Statistics of bacteria phyla and genera on the peanut shell. **Table S8.** Three core fungi OTUs in-the-shell and three core fungi OTUs on-the-shell. **Table S9.** 87 core bacterial OTUs on-the-shell. **Table S10.** Soil physical-chemical factor index and climate index. **Table S11.** Statistics of sequencing, assembly and gene sets. **Table S12.** Pathway enrichment of core KOs at the level 2 and level 3 classification of KEGG pathways. **Table S13.** Effects of soil physical-chemical and climatic factors on microbial functions. **Table S14.** All KO enrichment statistics. **Table S15.** KOs and metabolism pathways enriched significantly in Hong'an, Hubei province. **Table S16.** KOs and metabolism pathways enriched significantly in Zhangshu, Jiangxi province. **Table S17.** KOs and metabolism pathways enriched significantly in Zhanjiang, Guangdong province. **Table S18.** KOs and metabolism pathways enriched significantly in Tangshan, Hebei province. **Table S19.** KOs and metabolism pathways enriched significantly in Fuxin, Liaoning province. **Table S20.** KOs and metabolism pathways enriched significantly in Linyi, Shandong province. **Table S21.** Fungi and bacteria significantly associated with *Aspergillus flavus*. **Table S22.** Fungi and bacteria significantly associated with *Aspergillus flavus* and aflatoxin. **Table S23.** Fungi significantly associated with antagonistic *Exophiala*. **Table S24.** Fungi significantly associated with antagonistic *Trichoderma*. **Table S25.** Bacteria significantly associated with antagonistic *Bacillus*. **Table S26.** Functions (KOs) significantly correlated with *Aspergillus flavus*. **Table S27.** Statistics of functional classification significantly associated with *Aspergillus flavus*. **Table S28.** Enriched metabolism pathways on KEGG level 3 positively correlated with *Aspergillus flavus*. **Table S29.** Enriched metabolism pathways on KEGG level 3 negatively correlated with *Aspergillus flavus*.

References

1. Hacquard S, Garrido-Oter R, González A, Spaepen S, Ackermann G, Lebeis S, et al. Microbiota and host nutrition across plant and animal kingdoms. *Cell Host and Microbe*. 2015;17(5):603–16.
2. Finkel OM, Castrillo G, Herrera Paredes S, Salas González I, Dangl JL. Understanding and exploiting plant beneficial microbes. *Curr Opin Plant Biol*. 2017;38:155–63.
3. Edwards J, Johnson C, Santos-Medellín C, Lurie E, Podishetty NK, Bhatnagar S, et al. Structure, variation, and assembly of the root-associated microbiomes of rice. *Proc Natl Acad Sci U S A*. 2015;112(8):E911–20.
4. Lundberg DS, Lebeis SL, Paredes SH, Yourstone S, Gehring J, Malfatti S, et al. Defining the core *Arabidopsis thaliana* root microbiome. *Nature*. 2012;488(7409):86–90.
5. Castrillo G, Teixeira PJL, Paredes SH, Law TF, de Lorenzo L, Feltcher ME, et al. Root microbiota drive direct integration of phosphate stress and immunity. *Nature*. 2017;543(7646):513–8.
6. Berendsen RL, Vismans G, Yu K, Song Y, de Jonge R, Burgman WP, et al. Disease-induced assemblage of a plant-beneficial bacterial consortium. *ISME J*. 2018;12(6):1496–507.
7. Bulgarelli D, Schlaeppi K, Spaepen S, Ver Loren van Themaat E, Schulze-Lefert P. Structure and functions of the bacterial microbiota of plants. *Annu Rev Plant Biol*. 2013;64(1):807–38.
8. Roeland L, Berendsen GV, Ke Y, Yang S. Disease-induced assemblage of a plant-beneficial bacterial consortium. *ISME J*. 2018;12:1496–1507.
9. Yuan J, Zhao J, Wen T, Zhao M, Li R, Goossens P, et al. Root exudates drive the soil-borne legacy of above ground pathogen infection. *Microbiome*. 2018;6:156.
10. Fitzpatrick CR, Copeland J, Wang PW, Guttman DS, Kotanen PM, Johnson MTJ. Assembly and ecological function of the root microbiome across angiosperm plant species. *Proc Natl Acad Sci U S A*. 2018; 115 (6): E1157–65.
11. Klironomos JN. Feedback with soil biota contributes to plant rarity and invasiveness in communities. *Nature*. 2002;417(6884):67–70.
12. DA Inderjit W, Karban R, Callaway RM. The ecosystem and evolutionary contexts of allelopathy. *Trends Ecol Evol*. 2011;26(12):655–62.
13. Perez-Jaramillo JE, Carrion VJ, Bosse M, Ferrao LFV, de Hollander M, Garcia AAF, et al. Linking rhizosphere microbiome composition of wild and domesticated *Phaseolus vulgaris* to genotypic and root phenotypic traits. *ISME J*. 2017;11:2244–2257.
14. Wei Z, Yang T, Friman VP, Xu Y, Shen Q, Jousset A. Trophic network architecture of root-associated bacterial communities determines pathogen invasion and plant health. *Nat. commun*. 2015;6:8413.
15. Ioannis AS, Yu K, Kirstin F, Ronniede J. MYB72-dependent coumarin exudation shapes root microbiome assembly to promote plant health. *PNAS*. 2018;115:10.
16. Chen Y, Wang J, Yang N, Wen Z, Sun X, Chai Y, et al. Wheat microbiome bacteria can reduce virulence of a plant pathogenic fungus by altering histone acetylation. *Nat. commun*. 2018;9:3429.
17. Alison E, Bennett DG, Jason K, Sandra C, Claire H. Plant lignin content altered by soil microbial community. *NewPhytol*. 2015;206:166–174.
18. Liu X. Strengthen research work of exposure and control of mycotoxin. *Chinese journal of preventive medicine*. 2006; 40:307-308.
19. Mangan SA, Schnitzer SA, Herre EA, Mack KML, Valencia MC, Sanchez EI, et al. Negative plant–soil feedback predicts tree-species relative abundance in a tropical forest. *Nature*. 2010;466:752.
20. Amundson R, Berhe AA, Hopmans JW, Olson C, Szejn AE, Sparks DL, et al. Soil science. Soil and human security in the 21st century. *Science*. 2015; 348(6235):1261071.
21. Berendsen RL, Pieterse CMJ, Bakker PAHM. The rhizosphere microbiome and plant health. *Trends Plant Sci*. 2012;17:478–486.
22. Ding X, Li P, Bai Y, Zhou H. Aflatoxin B1 in post-harvest peanuts and dietary risk in China. *Food Control* 2012;23:143-148.
23. Nakai VK, Rocha LD, Gonzalez E, Fonseca H, Ortega EMM, Correa B. Distribution of fungi and aflatoxins in a stored peanut variety. *Food Chem*. 2008;106:285-290.
24. Ding N, Xing F, Liu X, Selvaraj JN, Wang L, Zhao Y, et al. Variation in fungal microbiome (mycobiome) and aflatoxin in stored in-shell peanuts at four different areas of China. *Front. Microbiol*. 2015;6:1055.
25. Xing FG, Ding N, Liu X, Selvaraj JN, Wang L, Zhou L, et al. Variation in fungal microbiome (mycobiome) and aflatoxins during simulated storage of in-shell peanuts and peanut kernels. *Scientific reports*. 2016; 6:25930.
26. Li A, Yao Y, Zhang L, Xiao J, Zhou X, Zhang X, et al. Analysis of Classification of Soil Fungi in Main Peanut Production Areas in China. *Journal of Peanut Science*. 2016; 45(1): 20-23.
27. Yao Y, Zhang L, Zheng B, Zhang J, Dong L, Xing A, et al. Screening of Peanut Endophytic Bacterial Antagonists against *Aspergillus flavus*, and Identification and antagonistic Activities of Strain B85-1. *Journal of Peanut Science*, 2016; 45(3): 25-26.
28. Yao Y, Ding D, Zhang Y, Chang X, Dong L, Zhang L, et al. Screening of Maize Endophytic Antagonists against *Aspergillus flavus* and Activities research of Antagonistic Strain B42-3. *Journal of the Chinese Cereals and Oils Association*. 2018; 33(3):85-88.
29. Chen Y, Liao C, Lin H, Chiueh L, Shih DYC. Survey of aflatoxin contamination in peanut products in Taiwan from 1997 to 2011. *J Food Drug Anal*. 2011;21:247-252.
30. Passone MA, Rosso LC, Ciancio A, Etcheverry M. Detection and quantification of *Aspergillus section Flavi* spp. in stored peanuts by real-time PCR of *nor-1* gene, and effects of storage conditions on aflatoxin production. *Int. J. Food Microbiol*. 2010;138:276–281.
31. Barros G, Torres A, Palacio G, Chulze S. *Aspergillus* species from section *Flavi* isolated from soil at planting and harvest time in peanut-growing regions of Argentina. *J. Sci. Food Agric*. 2003;83:1303–1307.

32. Francesca M, Ramona M, Marco F, Barbara S. The stage of soil development modulates rhizosphere effect along a High Arctic desert chronosequence. *ISME J.* 2018;12:1188–1198.
33. Devin CD, Damaris D, Citlali FG, Stephen G. Plant compartment and biogeography affect microbiome composition in cultivated and native *Agave* species. *New Phytol.* 2016;209:798–811.
34. Dan N, Stephanie DG, Elizabeth P, Devin CD. Drought and host selection influence bacterial community dynamics in the grass root microbiome. *ISME J.* 2017;11:2691–2704.
35. Taş N, Prestat E, Wang S, Wu YX, Ulrich C, Kneafsey T. Land scape topography structures the soil microbiome in arctic polygonal tundra. *Nat. commun.* 2018;9:777.
36. Chen Y, Wang J, Yang N, Wen Z, Sun X, Chai Y. Wheat microbiome bacteria can reduce virulence of a plant pathogenic fungus by altering histone acetylation. *Nat. commun.* 2018;9:3429.
37. Lammel D, Barth G, Ovaskainen O, Cruz L, Zanatta J, Ryo M. Direct and indirect effects of a pH gradient bring insights into the mechanisms driving prokaryotic community structures. *Microbiome.* 2018;6:106.
38. Owen GO, Rishi DK, Martin I, Bidartondo IH. Arbuscular mycorrhizal fungi promot coexistence and niche divergence of sympatric palm species on a remote oceanic is land. *New Phytol.* 2018;217:1254–1266 .
39. Maya OL, Noa S, Milana GV, Stefan JG. Niche and host-associated functional signatures of the root surface microbiome. *Nat. commun.* 2014;5:4950.
40. Zhang Y, Xu J, Riera N, Tao J, Li J, Zhang K, et al. Huanglongbing impairs the rhizosphere-to- rhizoplane enrichment process of the citrus root-associated microbiome. *Microbiome.* 2017;5:97.
41. Emilie C, Rodrigo M, Peter AHM, Jos MR. Fungal invasion of the rhizospher microbiome. *ISME. J.* 2016;10:265–268.
42. Bokulich NA, Subramanian S, Faith JJ, Gevers D, Jeffrey I Gordon JI, et al. Quality-filtering vastly improves diversity estimates from Illumina amplicon sequencing. *Nat Methods.* 2013;10:57-59.
43. Magoc T, Salzberg SL. FLASH: fast length adjustment of short reads to improve genome assemblies. *Bioinformatics.* 2011;27:2957-2963.
44. Caporaso JG, Kuczynski J, Stombaugh J, Bittinger K, Bushman FD, Costello EK, et al. QIIME allows analysis of high-throughput community sequencing data. *Nat Methods.* 2010;7:335-336.
45. Edgar RC. UPARSE: highly accurate OTU sequences from microbial amplicon reads. *Nat Methods.* 2013;10:996-998.
46. Edgar R. Taxonomy annotation and guide tree errors in 16S rRNA databases. *Peer J.* 2018;6:5030.
47. Quast C, Pruesse E, Yilmaz P, Gerken J, Schweer T, Yarza P, et al. The SILVA ribosomal RNA gene database project: improved data processing and web-based tools. *Nucleic Acids Res.* 2013;41:590-596.
48. Koljalg, U, Nilsson RH, Abarenkov K, Tedersoo L, Taylor AFS, Bahram M, et al. Towards a unified paradigm for sequence-based identification of fungi. *Mol Ecol.* 2013;22:5271-5277.
49. Chen J, Bittinger K, Charlson Emily S, Hoffmann C, Lewis J, Wu G, et al. Associating microbiome composition with environmental covariates using generalized UniFrac distances. *Bioinformatics.* 2012;28:2106-2113.
50. Lozupone C, Knight R. UniFrac: a new phylogenetic method for comparing microbial communities. *Appl Environ Microbiol.* 2005;71:8228-8235.
51. Kruskal JB. Multidimensional scaling by optimizing goodness of fit to a nonmetric hypothesis. *Psychometrika.* 1964;29:1-27.
52. Oksanen J, Minchin PR. Instability of ordination results under changes in input data order: explanations and remedies. *J Veg Sci.* 1997;8:447-454.
53. Li, D, Luo R, Liu C, Leung C, Ting H. MEGAHIT v1.0: A Fast and Scalable Metagenome Assembler driven by Advanced Methodologies and Community Practices. *Methods.* 2016;102:3-11.
54. Li, D, Luo R, Liu C, Sadakane K, Lam TW. MEGAHIT: an ultra-fast single-node solution for large and complex metagenomics assembly via succinct de Bruijn graph. *Bioinformatics.* 2015;31:1674-1676.
55. Zhu W, Lomsadze A, Borodovsky M. Ab initio gene identification in metagenomic sequences. *Nucleic Acids Res.* 2010;38:132.
56. Besemer J, Borodovsky M. Heuristic approach to deriving models for gene finding. *Nucleic Acids Res.* 1999; 27:3911-3920.
57. Li W, Adam G. Cd-hit: a fast program for clustering and comparing large sets of protein or nucleotide sequences. *Bioinformatics.* 2006;22:1658.
58. Fu L, Niu B, Zhu Z, Wu S, Li W. CD-HIT: accelerated for clustering the next-generation sequencing data. *Bioinformatics.* 2012;28:3150-3152.
59. Qin J, Li Y, Cai Z, Li S, Zhu J, Zhang F, et al. A metagenome-wide association study of gut microbiota in type 2 diabetes. *Nature.* 2012;490:55-60.
60. Buchfink B, Xie C, Huson DH. Fast and sensitive protein alignment using DIAMOND. *Nat Methods.* 2015;12:59-60.
61. Kanehisa M, Goto S, Hattori M, Aoki-Kinoshita K, Itoh M, Kawashima S et al. From genomics to chemical genomics: new developments in KEGG. *Nucleic Acids Res.* 2006;34:354-357.
62. Kanehisa M, Goto S, Kawashima S, Okuno Y, Hattori M, Kanehisa M. The KEGG resource for deciphering the genome. *Nucleic Acids Res.* 2004;32:277-280.
63. Zhu L, Dong Y, Jin W, Wang C, Chen Y. Study on Soil Physical and Chemical Properties of ZhoushanIsland and Outlying Islands. *Zhejiang chemical industry.* 2019; 15(7): 47-54.
64. Zhang M, Wang L, Cheng X, Wang Y, Zhang J. Application of External Heating Digestion-Air Cooled Tube Reflow in the Determination of Soil Organic Matter Content. *Contemporary Chemical Industry.* 2019; 48(9): 2129-2131.
65. Wolfe MH, Nonparametric DA. *Statistical Methods.* New York: John Wiley & Sons (1973).
66. Benjamini Y, Hochberg Y. Controlling the False Discovery Rate: A Practical and Powerful Approach to Multiple Testing. *J R Stat Soc.* 1995;57:289-300.
67. Love MI, Huber W, Anders S. Moderated estimation of fold change and dispersion for RNA-seq data with DESeq2. *Genome Biol.* 2014;15:550.

Figures

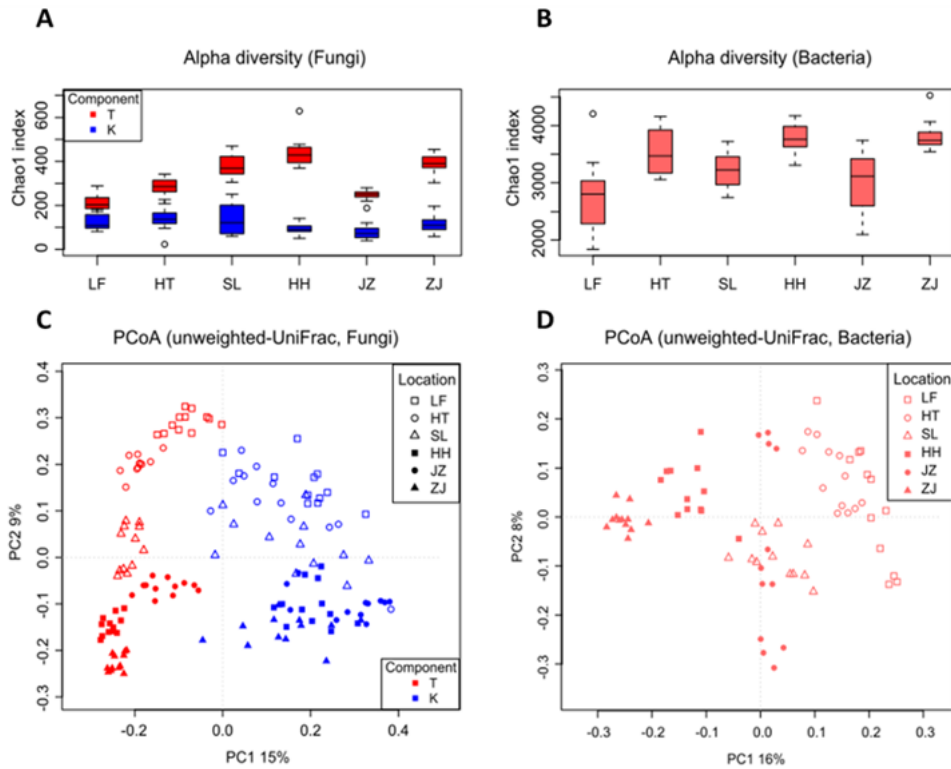


Figure 1
 Diversity of microbiota associated with peanut shells in the 6 major planting areas. a Alpha diversity of on-the-shell-surface and in-the-shell fungi associated with peanuts. b Alpha diversity of on-the-shell-surface bacteria associated with peanuts. c PCoA analysis of fungal community structure associated with peanuts. d PCoA analysis of bacterial community structure associated with peanuts. Red depicts on-the-surface-of-shell samples (T), blue depicts in-the-peanut-shell samples (K), the hollow symbols are the low aflatoxin areas samples, and the solid symbols are the high aflatoxin areas samples. LF depicts samples collected in Fuxin of Liaoning province, HT depicts samples collected in Tangshan from Hebei province, SL depicts samples collected in Linyi of Shandong province, HH depicts samples collected in Hong'an from Hubei province, JZ depicts samples collected in Zhangshu from Jiangxi province, ZJ depicts samples collected in Zhanjiang from Guangdong province.

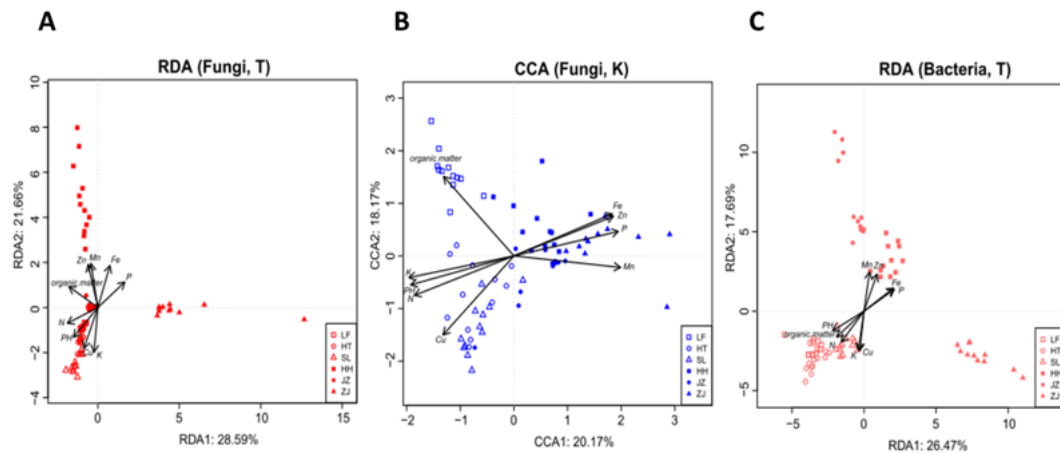


Figure 2
 Effects of physical and chemical factors of soil on the structure of fungi associated with peanuts. a RDA clustering of ITS data from on-the-shell-surface samples and environmental factors. b CCA clustering of ITS data from in-the-shell samples and environmental factors. c RDA clustering of 16S data from the on-the-shell-surface samples and environmental factors.



Figure 3

KEGG pathways enriched by on-the-shell-surface or in-the-shell samples. The abscissa represents the enrichment index, the ordinate represents the path name. Greater than 1.7 indicates enriched pathways in the low aflatoxin areas, less than 1.7 represents enriched pathways in the high aflatoxin regions. Color represents the first-level functional classification of individual pathway. Bubble size represents relative enrichment index.

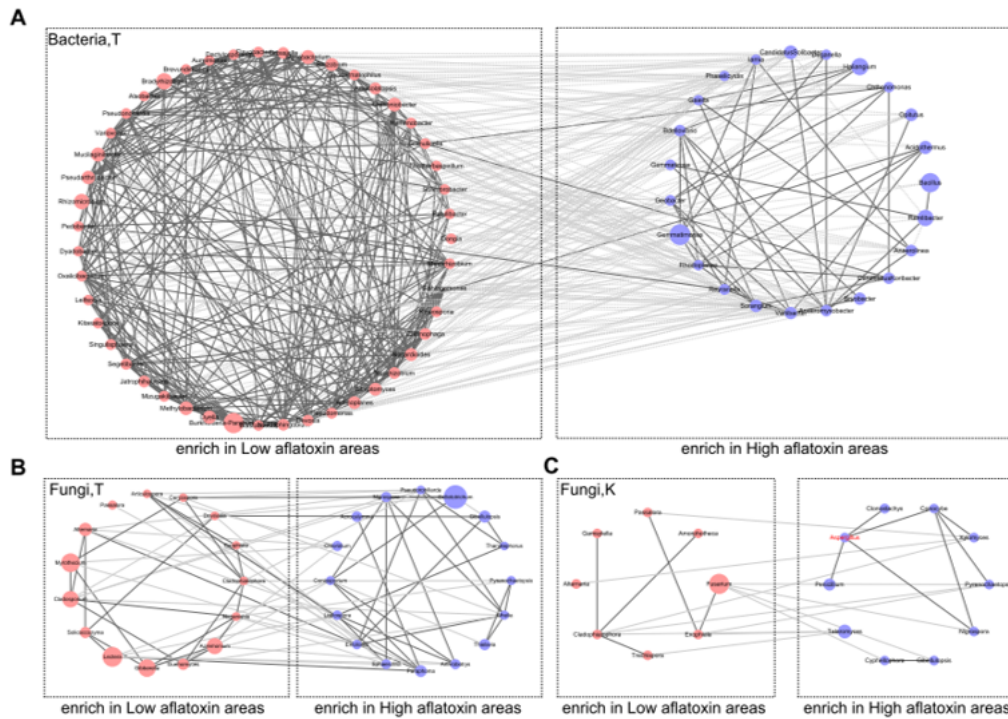


Figure 4

Correlation network diagram of *Aspergillus flavus* and peanut pod-associated microbial populations. a Network diagram based on the bacterial genus level (in the shell). b Network diagram based on fungal genus level (on the surface of shell). c Network map based on fungal genus level (in the shell). Red dots indicate species significantly enriched in the low aflatoxin areas, blue dots indicate species significantly enriched in the high aflatoxin areas. The solid line indicates a positive correlation and the dashed line indicates a negative correlation. The size of the dots represents the average abundance of the species. Selection criteria: the average abundance of species is higher than 0.1%, and the correlation between species is significant, higher than 0.35 or lower than -0.35.

Spearman correlation

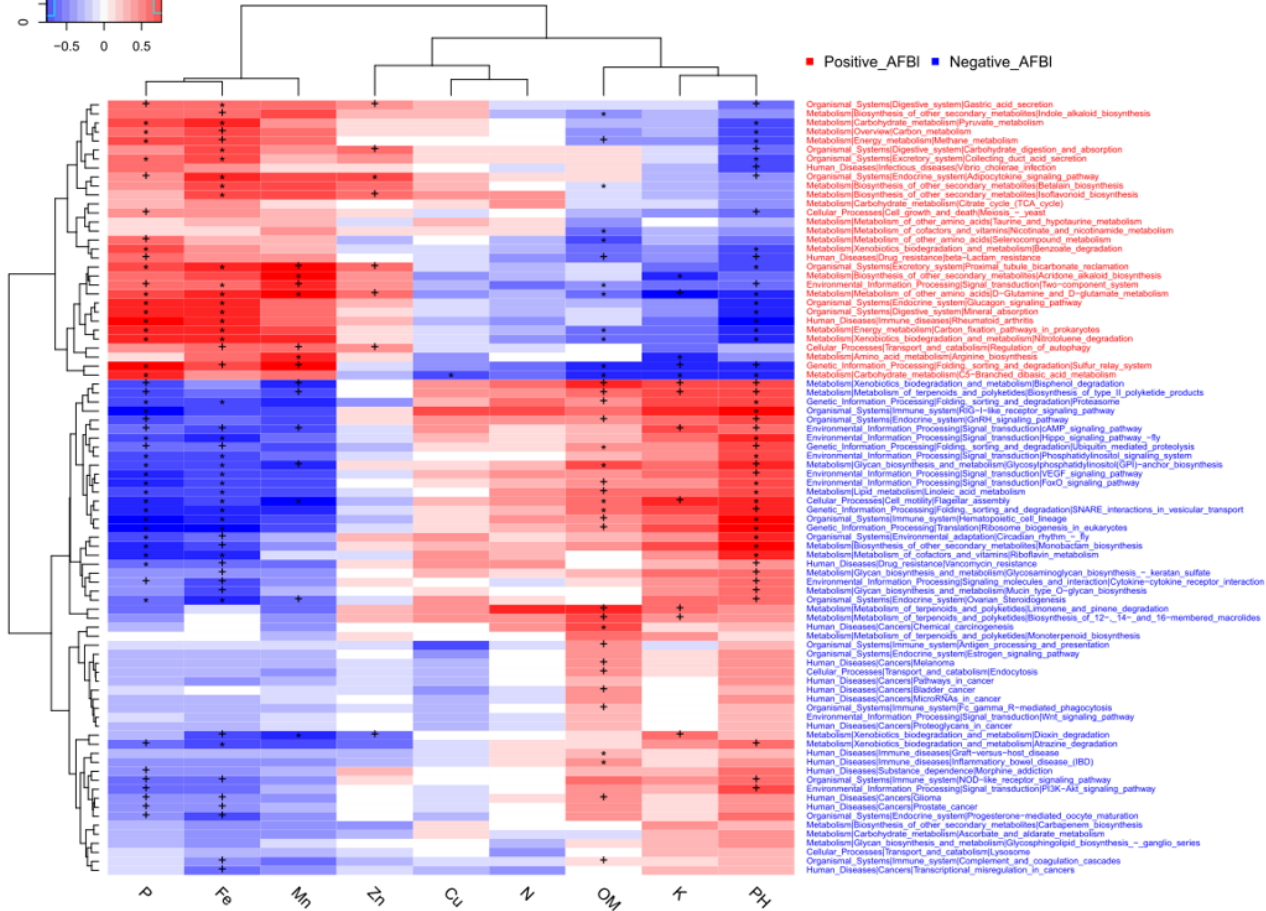
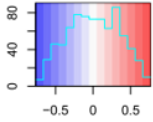


Figure 5

Correlation analysis of aflatoxin-related KOs (positive and negative) and soil physical and chemical indicators (permanova). positive_AFB1 means a pathway with a significant positive correlation with aflatoxin, and Negative_AFB1 means a significantly negative correlation with aflatoxin pathway.

Supplementary Files

This is a list of supplementary files associated with this preprint. Click to download.

- [Supplementaltables.xls](#)